Loss-of-Function and Gain-of-Function Mutations in *KCNQ5* Cause Intellectual Disability or Epileptic Encephalopathy

Anna Lehman,[1,*] Samrat Thouta,[2] Grazia M.S. Mancini,[3] Sakkubai Naidu,[4] Marjon van Slegtenhorst,[3] Kirsty McWalter,[5] Richard Person,[5] Jill Mwenifumbo,[1] Ramona Salvarinova,[6] CAUSES Study,[7] EPGEN Study,[7] Ilaria Guella,[8] Marna B. McKenzie,[8] Anita Datta,[9] Mary B. Connolly,[9] Somayeh Mojard Kalkhoran,[2] Damon Poburko,[2] Jan M. Friedman,[1] Matthew J. Farrer,[1,8] Michelle Demos,[9] Sonal Desai,[4] and Thomas Claydon[2,*]

KCNQ5 is a highly conserved gene encoding an important channel for neuronal function; it is widely expressed in the brain and generates M-type current. Exome sequencing identified de novo heterozygous missense mutations in four probands with intellectual disability, abnormal neurological findings, and treatment-resistant epilepsy (in two of four). Comprehensive analysis of this potassium channel for the four variants expressed in frog oocytes revealed shifts in the voltage dependence of activation, including altered activation and deactivation kinetics. Specifically, both loss-of-function and gain-of-function *KCNQ5* mutations, associated with increased excitability and decreased repolarization reserve, lead to pathophysiology.

Introduction

Potassium channels are ubiquitous in all eukaryotic cells and serve multiple roles, including maintenance of cell osmolality and volume, control of cell-membrane potentials, and propagation of electrical signals in nerve cells.[1] The largest and most diverse group of ion channels, potassium channels, are tetrameric and span the lipid bilayer of the cell membrane. Action potentials in nerve cells occur via a process of polarization and repolarization, which is modulated by many different subtypes of potassium channels. Each channel subtype has its own profile of kinetics, voltage dependence, and sensitivity to pharmacologic blocking agents. More than 90 human genes encode potassium channel subunits with variable expression across tissue types, and more than one-third of these genes are known to cause human diseases when mutated. Review of Online Mendelian Inheritance in Man reveals that the range of clinical effects in various tissues is broad and includes cardiac arrhythmia (e.g., *KCNE1* [MIM: 176261], *KCNE2* [MIM: 603796], *KCNH2* [MIM: 152427], and *KCNJ2* [MIM: 600681]), sensorineural hearing impairment (e.g., *KCNE1*, *KCNQ1* [MIM: 607542], and *KCNQ4* [MIM: 603537]), retinopathy (e.g., *KCNJ13* [MIM: 603208] and *KCNV2* [MIM: 607604]), pulmonary hypertension (*KCNK4* [MIM: 605720]), insulin-secretion defects (e.g., *KCNJ11* [MIM: 600937]), hyperaldosteronism (*KCNJ5* [MIM: 600734]), Bartter syndrome (*KCNJ1* [MIM: 600359]), dehydrated hereditary stomatocytosis (*KCNN4* [MIM: 602754]), episodic ataxia (*KCNA1* [MIM: 176260]), spinocerebellar ataxia (*KCNC3* [MIM: 176264] and *KCND3* [MIM: 605411]), epilepsy (e.g., *KCNB1* [MIM: 600397], *KCNC1* [MIM: 176258], *KCNMA1* [MIM: 600150], *KCNQ2* [MIM: 602235], *KCNQ3* [MIM: 602232], and *KCNT1* [MIM: 608167]), and intellectual disability (e.g., *KCNA2* [MIM: 176262], *KCNA4* [MIM: 176266], *KCNH1* [MIM: 603305], *KCNJ6* [MIM: 600877], *KCNJ10* [MIM: 602208], *KCNK9* [MIM: 605874], and *KCNQ2*).

Voltage-gated potassium channels Kv7.1–Kv7.5 are encoded by *KCNQ1–KCNQ5* (MIM: 607357), respectively. Bi-allelic loss-of-function mutations in *KCNQ1* cause Jervell and Lange-Nielsen syndrome (sensorineural hearing impairment with arrhythmia [MIM: 220400]), and heterozygous mutations can cause a range of cardiac arrhythmias or alter insulin secretion.[2–4] *KCNQ2* and *KCNQ3* heterodimerize with one another; heterozygous mutations in either gene can result in benign familial neonatal seizures (MIM: 121200 and 121201) or epileptic encephalopathy (MIM: 613720).[5–7] There is evidence that Kv7.5 subunits can heterodimerize with Kv7.3 subunits.[8] Mutations in *KCNQ4* can cause autosomal-dominant sensorineural hearing impairment.[9]

Material and Methods

Mutation of *KCNQ5* was independently identified as a candidate cause of intellectual disability or epileptic encephalopathy by

[1]Department of Medical Genetics, University of British Columbia, Vancouver, BC V6H 3N1, Canada; [2]Department of Biomedical Physiology and Kinesiology, Simon Fraser University, Burnaby, BC V5A 1S6, Canada; [3]Department of Clinical Genetics, Erasmus University Medical Center, 3000 CA Rotterdam, the Netherlands; [4]Department of Neurogenetics, Kennedy Krieger Institute, Baltimore, MD 21211, USA; [5]GeneDx, Gaithersburg, MD 20877 USA; [6]Division of Biochemical Diseases, Department of Pediatrics, University of British Columbia, Vancouver, BC V6H 3N1, Canada; [7]University of British Columbia, Vancouver, BC V6H 3N1, Canada; [8]Centre for Applied Neurogenetics, University of British Columbia, Vancouver BC, V6T 1Z3, Canada; [9]Division of Pediatric Neurology, Department of Pediatrics, University of British Columbia, Vancouver BC, V6H 3N1, Canada
*Correspondence: alehman@cw.bc.ca (A.L.), thomas_claydon@sfu.ca (T.C.)
http://dx.doi.org/10.1016/j.ajhg.2017.05.016.

four sequencing providers for four probands. GeneMatcher postings, and subsequent communications, enabled independent discoveries to be corroborated.[10] Written informed consent for exome sequencing and approval by ethics review boards were obtained from Erasmus Medical Center (protocol MEC-2012387) for individual 1 and from the University of British Columbia (protocols H-15-00092, H-09-01228, and H-14-01531) for individuals 2 and 4. Individual 3 received sequencing through clinical care, and written informed consent was obtained for publication of medical history.

For individual 1, genomic DNA was isolated from peripheral blood of the proband, mother, and father, and exome-coding DNA was captured with the Agilent Sure Select Clinical Research Exome Kit. Reads were aligned to UCSC Genome Browser build hg19 with the Burrows-Wheeler Aligner (BWA-MEM v.0.7.5a, and variants were called with the Genome Analysis Toolkit HaplotypeCaller (v.2.7-2). Detected variants were annotated, filtered, and prioritized with the Bench Lab NGS v.3.1.2 platform (Cartagenia). Individual 2 was exome sequenced through the CAUSES (Clinical Assessment of the Utility of Sequencing and Evaluation as a Service) study—a translational research study seeking to apply exome sequencing as a hospital-based programmatic service. Genomic DNA was isolated from peripheral blood of the proband, mother, and father, and exome-coding DNA was captured with the Agilent Sure Select All Exon V5+UTR Kit. The products were sequenced on the Illumina HiSeq 2500 with v.4 chemistry. A customized bioinformatics pipeline,[11] coupled with visual validation (Integrative Genomics Viewer), identified variants of interest. Individual 3 underwent trio-based Illumina exome sequencing at GeneDx, a diagnostic laboratory certified by the College of American Pathologists and Clinical Laboratory Improvement Amendments. Genomic DNA was extracted from whole blood from the affected child and parents. Exon targets were isolated with the Clinical Research Exome (Agilent Technologies). Additional sequencing technology and a variant-interpretation protocol have been previously described.[12] The general assertion criteria for variant classification are publicly available on the GeneDx ClinVar submission page. Individual 4 was enrolled in the Epilepsy Genetics Study (EPGEN)—a clinical genetic study seeking to assess the utility and economy of exome-based diagnostics in optimizing management of early-onset epilepsy. Trio-based exome sequencing was performed on DNA extracted from peripheral-blood lymphocytes with the Ion AmpliSeq Exome Kit (57.7 Mb) and Ion Proton System, and then genes linked or associated with seizure disorders underwent bioinformatics analysis and prioritization.[13] Variants were confirmed with Sanger sequencing. Primer sequences are available upon request. *KCNQ5* variants were annotated on GenBank: NM_001160133 (hg19).

Open-reading-frame full-length human cDNA sequences (GenBank: NM_001160133) were custom synthesized (GENEWIZ). Whole-cell membrane current recordings from *Xenopus* oocytes expressing wild-type (WT) or mutant Kv7.5 constructs were collected with a two-electrode voltage clamp and an OC-725C amplifier (Warner Instruments). Signals were digitized and acquired with a Digidata 1440 A/D converter and pClamp 10.2 software (Axon Instruments). Recordings were performed at 20°C–22°C, and oocytes were perfused with ND96 solution (96 mM NaCl, 3 mM KCl, 0.5 mM $CaCl_2$, 1 mM $MgCl_2$, and 5 mM HEPES titrated to pH 7.4 with NaOH) at 1 mL/min. For measurement of activation properties, oocytes were held at −100 mV and subjected to 3 s depolarizing steps to 50 mV in 10 mV increments. Instantaneous tail currents recorded during a subsequent 1 s step to −30 mV were used for generating conductance-voltage (G-V) relationships. G-V relationships were described by the Boltzmann equation: $y = 1/(1 + \exp(V_{1/2} - V)/k)$, where y is the relative conductance normalized to the maximum conductance (G/Gmax), $V_{1/2}$ is the voltage at which half maximal conductance was recorded, V is the test voltage, and k is the slope factor. We determined activation and deactivation kinetics by fitting the rise in current upon depolarization (activation) and current decay upon repolarization (deactivation) with an exponential function at a range of voltages. Data were analyzed with Clampfit 10.3 (Axon Instruments) and SigmaPlot11 (Systat Software). Data are presented as the mean ± SEM. The value n represents the number of oocytes tested. Statistical significance was evaluated with a one-way or two-way ANOVA followed by a Bonferroni post-test for multiple comparisons.

Two approaches were taken for determining relative expression levels of mutant channels. In the first, peak current amplitude at +40 mV was compared between mutant and WT channels at the same time of day in the same batch of oocytes injected with the same amount of cRNA. In the second approach, cell expression of each construct was evaluated by immunocytochemistry. HEK293 cells were plated on 12 mm glass coverslips and were transfected with 1 μg of the channel cDNA in pCNDA3.1. All solutions for immunohistochemistry were made in Dulbecco's phosphate-buffered solution. Approximately 24 hr after transfection, cells were fixed with 4% paraformaldehyde (room temperature, 15 min), permeabilized with 0.1% Triton X-100, blocked with 4% normal goat serum (1 hr), and stained overnight at 4°C with anti-Kv7.5 (1:500; C-terminal epitope, aa 880–897, Thermo Fisher Scientific). The following day, cells were labeled with Alexa Fluor 647 Goat anti-Rabbit IgG (H+L) secondary antibody (1:500; A-21245, Thermo Fisher Scientific), stained with Hoescht 33342 (1 μg/mL), and mounted in ProLong Gold. z stacks were acquired at 0.2 μm steps on an inverted Nikon TiE epifluorescence microscope with a Zyla 5.5 camera (Andor) and a CFI Plan Apo Lambda 100× 1.45 NA objective. Images were analyzed with Fiji. Kv7.5 images were background subtracted with a 600 nm rolling ball before generation of a maximal intensity projection of the three slices closest to the coverslip for best estimation of cell surface expression. Hand-drawn regions of interest were analyzed in two to five fields of view per Kv7.5 variant. One-way ANOVA of mean fluorescence intensity of labeling was performed in JMP (v.12. SAS Institute).

Results

Two probands with non-syndromic intellectual disability (individuals 2 and 3) and two with epileptic encephalopathy (individuals 1 and 4) were identified as each having a different heterozygous de novo missense variant in *KCNQ5* (GenBank: NM_001160133.1 and NP_001153604): c.1343G>T (p.Ser448Ile) in individual 1, c.434T>G (p.Val145Gly) in individual 2, c.1021C>A (p.Leu341Ile) in individual 3, and c.1106C>G (p.Pro369Arg) in individual 4. Each of these variants was absent from gnomAD, and each was associated with a high REVEL score (0.782 for c.1343G>T, 0.886 for c.434T>G, 0.827 for c.1021C>A, and 0.918 for c.1106C>G).[14] Additional in silico prediction programs

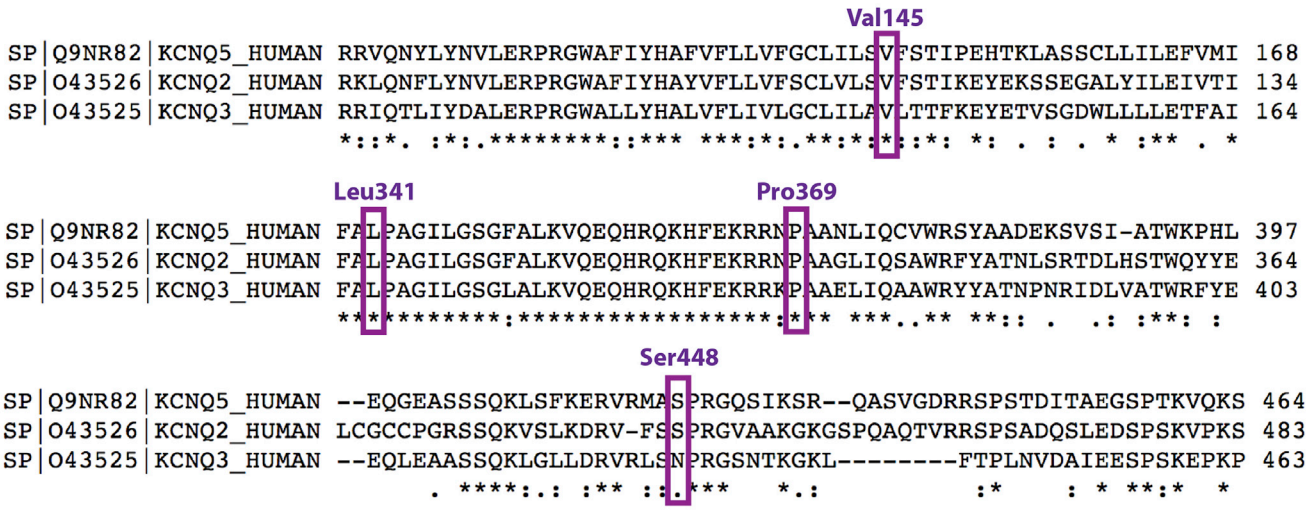

Figure 1. Partial Clustal Omega Alignments of Kv7.5, Kv7.2, and Kv7.3
Residues with missense variants in the subject cohort are labeled and boxed. UniProt identifiers are labeled to the left of the protein name; note that the numbering of UniProt: Q9NR82 for Kv7.5 is different for Ser448 than the numbering of the canonical GenBank: NP_001153604, referred to elsewhere in this manuscript. These residues are strongly constrained, although Kv7.3 features an alternate amino acid for Ser448. In its entirety, Kv7.5 shares 50% identity with Kv7.2 and Kv7.3.

(SIFT, MutationTaster, and PROVEAN) consistently indicated that all four mutations would most likely be damaging to the protein, except that PROVEAN predicted c.1343G>T (p.Ser448Ile) to be neutral. An alignment with Kv7.5's paralogs, Kv7.2 and Kv7.3, also showed strong expression in the brain, revealing that their encoding residues are uniformly maintained, except that an asparagine replaces a serine at position 448 in KCNQ3 (Figure 1). *KCNQ5* demonstrates general intolerance of both missense mutations and haploinsufficiency, as indicated by a *Z* score of 4.62 for the former and a pLI score of 1.0 for the latter in the Exome Aggregation Consortium (ExAC) Browser.[15] All variants were confirmed to be de novo in probands (absent in parents) by Sanger capillary sequencing.

There were no suspicious variants of interest in individuals 1, 3, or 4 in addition to de novo variants in *KCNQ5*. An additional maternally inherited variant of uncertain significance (c.214C>G [p.Glu72Gln]) was identified in *SYP* on chromosome X in individual 2 (male). The phenotype associated with *SYP* loss of function appears to be non-syndromic intellectual disability.[16] This variant is not reported in public databases, but two hemizygotes for a different change at the same residue, p.Glu72Lys, are recorded in gnomAD.[15] Furthermore, the composite REVEL score is low (0.232), suggesting that the variant is likely to be non-damaging.

Comparison of phenotypes showed similarities among the four individuals, including absence of dysmorphic features, hypotonia, intellectual disability, and impaired coordination or unsteady gait (Table 1). Individuals 2 and 4 both had treatment-resistant epilepsy, and individual 4 had the additional feature of cortical atrophy, along with a greater degree of neurological impairment and being non-ambulatory and dependent on a jejunostomy tube for nutrition. At 5 months of age, individual 4 developed infantile spasms with hypsarrhythmia on electroencephalography (EEG) and an electrodecremental pattern during epileptic spasms. Spasms were unresponsive to vigabatrin, adrenocorticotropic hormone (ACTH), prednisone, and pyridoxine. She subsequently developed myoclonic-tonic, myoclonic, and tonic seizures. The following therapies were ineffective: topiramate, lamotrigine, phenobarbital, valproic acid, nitrazepam, clobazam, clonazepam, levetiracetam, piracetam, ethosuximide, sulthiame, carbamazepine, oxcarbazepine, acetazolamide, lacosamide, rufinamide, gabapentin, and the ketogenic diet. The longest seizure-free period was 2 weeks on ACTH. Hypsarrhythmia persisted for several months, and EEG evolved to a pattern with no posterior dominant rhythm, generalized delta activity, generalized sharp-and-slow-wave complexes, or multifocal sharp waves and spikes. Seizures characterized by a myoclonic jerk followed by generalized body and limb stiffening and eye deviation to the left were recorded in association with a generalized sharp wave followed by an electrodecremental pattern. Myoclonic seizures were recorded with generalized sharp waves. At the most recent follow-up at age 11 years, she was having multiple seizures daily and was on six anti-seizure medications.

Seizure types for individual 1 included absence and focal-onset seizures with impaired awareness. From the age of 2 years, he developed seizures initially characterized by short periods of staring, sometimes followed by extension of both arms, shouting, and focal limb jerks, without post-ictal phenomena; later in childhood, the attacks progressed to loss of consciousness and generalized tonic seizures. EEG confirmed diffuse epileptic activity. Despite treatment with valproate and lamotrigine, he continues to experience almost daily attacks of decreased awareness,

Table 1. Phenotypic Findings from Clinical Histories, Physical Examination, Brain Imaging, and EEG

	Individual 1	Individual 2 (CAUSES 053)	Individual 3	Individual 4 (EPGEN 013)
KCNQ5 variant (GenBank)	c.1343G>T (p.Ser448Ile) (NM_001160133)	c.434T>G (p.Val145Gly) (NM_001160133)	c.1021C>A (p.Leu341Ile) (NM_001160133)	c.1106C>G (p.Pro369Arg) (NM_001160133)
Age at last follow up	14 years	11 years	5 years	10 years
Family history	negative for neurodevelopmental disorders	negative for neurodevelopmental disorders	relatively uninformative, paternal cousin with developmental delay, ID, and microcephaly	negative for neurodevelopmental disorders
Ancestry	Southeast Asian	Southeast Asian	South Asian and European	Southeast Asian
Gender	male	male	male	female
Delivery	uncomplicated term SVD	uncomplicated term SVD	term C-section for signs of fetal distress	uncomplicated term C-section
Birth weight	3,430 g	3,402 g	unknown	3,060 g
Ambulation	unstable ataxic gait	achieved at 18 months, normal gait, unable to tandem walk	achieved at 18 months, walks on toes, unstable	nonambulatory
Language	no speech	simple sentences	limited speech	nonverbal
ID severity	severe	mild	mild to moderate	severe to profound
Seizures	from the age of 2 years, absence and focal-onset seizures with impaired awareness and uncontrolled by multiple AED	none	none	onset at 5 months, epileptic encephalopathy, infantile spasms followed by tonic seizures, treatment resistant
EEG	high voltage, diffusely slow background pattern, sharp waves and peak waves in frontal areas	normal EEG at age 11 years	normal	abnormal dysrhythmic background and multifocal epileptiform activity at age 9 years
Other neurological abnormalities	decreased deep tendon reflexes, mild hypotonia, pronounced sleepiness	non-REM parasomnias, hypotonia, incontinence	mild axial hypotonia	reduced visual attentiveness, axial hypotonia, spasticity in limbs
Brain MRI	normal at 7 years	normal at 9 years	normal at 3 years	progressive atrophy
Height	142 cm (−2 SD)	138.5 cm (−1.05 SD)	100 cm (−1.75 SD)	131 cm (−1.75 SD)
Weight	29 kg	25.1 kg	15.6 kg	26 kg
Head circumference	53 cm (−1 SD)	50 cm (−2 SD)	50.5 cm (−1 SD)	48.5 cm
Morphology	normal	normal	normal	normal
Other	none	two small simple cysts in left kidney	atopic dermatitis explained by an *FLG* variant on exome	fed via jejunostomy tube

Abbreviations are as follows: AED, anti-epileptic drug; EEG, electroencephalography; ID, intellectual disability; REM, rapid eye movement; and SVD, spontaneous vaginal delivery.

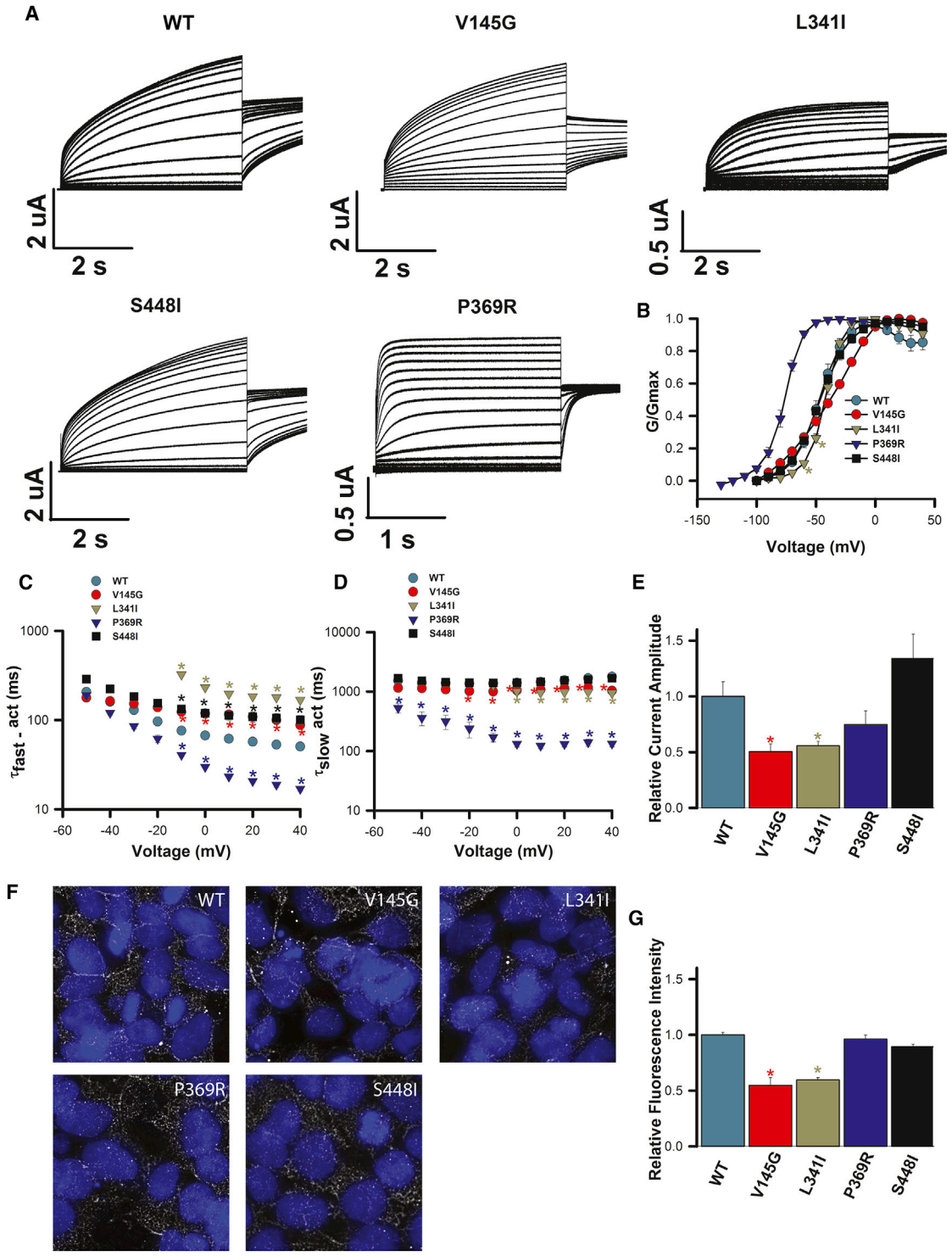

Figure 2. Heterologous Expression of Homomeric WT and Mutant Kv7.5 Channels

(A) Representative current traces for WT, p.Val145Gly (V145G), p.Leu341Ile (L341I), p.Ser448Ile (S448I), and p.Pro369Arg (P369R) Kv7.5 were recorded in *Xenopus laevis* oocytes during 3 s depolarizations from −100 to 40 mV in 10 mV increments, followed by a 1 s step to −30 mV. The holding potential was −100 mV.

(B) Conductance-voltage relationships for WT and mutant channels determined from instantaneous tail current amplitudes. Lines represent fits of the data with a Boltzmann function. $V_{1/2}$ and k values were −46.2 ± 1.8 mV and 10.8 ± 0.8 mV (n = 7) for the WT. Corresponding values were −38.8 ± 1.1 and 18.4 ± 0.2 mV (n = 7) for p.Val145Gly, −42.9 ± 1.2 and 7.0 ± 0.2 mV (n = 5) for p.Leu341Ile, −46.6 ± 1.1 and 12.3 ± 1.2 mV (n = 6) for p.Ser448Ile, and −77 ± 0.8 and 7.6 ± 0.3 mV (n = 5) for p.Pro369Arg.

(C and D) Activation kinetics for WT and mutant channels. Activating currents over a range of voltages were fitted to a double exponential function to yield values for τ_{fast} (C) and τ_{slow} (D) of activation. τ_{slow} values were largely voltage independent and unaffected by the variants, except for p.Pro369Arg.

(legend continued on next page)

shaking, facial cramps, and unnatural laughter. Sleep disturbance affects individuals 1 and 2.

We searched previously published datasets of large-scale sequencing studies on the causes of neurodevelopmental disability for other reports of de novo *KCNQ5* mutations and found c.867G>T (p.Lys289Asn), c.1328G>A (p.Arg443Gln), and c.1727A>G (p.His576Arg) in the supplemental data from 820 probands in Lelieveld et al.[17] However, these variants were not identified as candidate causes of neurodevelopmental disability in the course of the authors' statistical analyses. The largest currently published cohort of individuals with developmental disorders (the Deciphering Developmental Disorders study, n = 4,293) did not feature any *KCNQ5* de novo variants,[18] nor were any included in the data from the cohort of 2,508 autism probands from Iossifov et al.[19]

Because of the above evidence associating *KCNQ5* mutations with neurodevelopmental disorders, as well as prior evidence that mutations in *KCNQ2* (encoding Kv7.2) and *KCNQ3* (encoding Kv7.3) most likely cause neurological disease via reduced basal M-current (and subsequent neuronal hyperexcitability),[20] the impact of each mutation was characterized in vitro. Figure 2 shows that heterologous expression of homomeric WT Kv7.5 channels yielded voltage-dependent K^+ currents that activated slowly upon depolarization with a $V_{1/2}$ of activation of −46.2 ± 1.8 mV (n = 7), as has been described previously.[8,21] All four aberrant proteins exhibited robust functional expression when expressed as homomers. Compared with WT channels, each altered channel modified gating properties (Figures 2 and 3), and this was evident in the activation (Figure 2A) and deactivation (Figure 3A) current traces. The p.Val145Gly variant, located in the voltage-sensing unit of the channel (S1), led to subtle effects on channel function. The voltage dependence of activation was not significantly altered from that of the WT ($V_{1/2}$ = −38.8 ± 1.1 mV, n = 7; not significant [NS], ANOVA; Figure 2B). However, compared with WT channels, p.Val145Gly slowed early activation at depolarized voltages (Figure 2C) and deactivation kinetics (Figure 2B) across the entire voltage range tested ($p < 0.05$, two-way ANOVA; Figure 3B). In addition, p.Val145Gly reduced channel expression. Relative functional expression (Figure 2E) was reduced by 50% ± 7% (n = 7; $p < 0.01$), and immunocytochemistry labeling (Figures 2F and 2G) suggested that protein levels were reduced by 45% ± 7% ($p < 0.05$). Compared with the WT, p.Leu341Ile (S6, pore domain) did not alter the $V_{1/2}$ of activation ($V_{1/2}$ = −42.1 ± 1.2 mV, n = 5; NS, ANOVA; Figure 2B); however, activation in the subthreshold range of the action potential (−60 and −50 mV) was shifted to more depolarized potentials. Furthermore, compared with WT channels, p.Leu341Ile channels slowed the early phase of activation (Figure 2C) and deactivation kinetics (Figure 3B) at all voltages ($p < 0.05$, two-way ANOVA). Moreover, in a manner similar to p.Val145Gly, p.Leu341Ile reduced functional channel expression (Figure 2E) by 45% ± 5% (n = 9; $p < 0.05$) and protein immunolabeling (Figures 2F and 2G) by 40% ± 2%. Like p.Val145Gly, p.Ser448Ile (C terminal) channel function was subtly altered. Activation kinetics were significantly slower than those of WT channels at depolarized potentials ($p < 0.05$, two-way ANOVA; Figure 2C), although no differences were observed in the voltage dependence of activation or the kinetics of deactivation (Figures 2B and 3B). Channel expression was also not affected. The functional expression level relative to the WT level was 130% ± 22% (n = 6, NS; Figure 2E), and immunolabeling showed protein levels to be not significantly different from those of WT Kv7.5 (Figures 2F and 2G). In contrast, p.Pro369Arg (C terminus) shifted the voltage dependence of activation by ∼30 mV in the hyperpolarizing direction ($V_{1/2}$ = −77.0 ± 0.8 mV, n = 5; $p < 0.05$, ANOVA; Figure 2B). Corresponding to this pronounced shift, the kinetics of both early and late phases of activation were significantly accelerated ($p < 0.05$, two-way ANOVA; Figures 2C and 2D). Deactivation kinetics were slowed by the variant (Figure 3B). Channel expression was not affected by the variant. The functional expression level relative to the WT level was 74% ± 12% (n = 6, NS; Figure 2E), and immunolabeling of protein levels was not different from that of WT Kv7.5 (Figures 2F and 2G).

Discussion

Mutations in *KCNQ5* (encoding Kv7.5) can result in a congenital neurological disorder with intellectual disability or epileptic encephalopathy. Mutations in other *KCNQ* homologs, *KCNQ2* and less commonly *KCNQ3*, can also result in epilepsy either by loss-of-function or by gain-of-function effects.[7,22–24] In neurons, Kv7.5 is important for regulation of the M-type current, and hence firing rates. The M-current is a slowly activating and deactivating neuronal potassium current that plays a crucial role in regulating neuronal excitability by impeding repetitive

(E) Relative functional channel expression. Mean current amplitudes of homomeric WT and mutant Kv7.5 channels were compared at the end of a 3 s voltage step to +40 mV. Current amplitudes from mutant channels were normalized to the current amplitude of WT Kv7.5 channels recorded from oocytes injected with the same amount of cRNA on the same day. A t test with day as a blocking factor and mutant as a treatment factor was used to compare mutant and WT expression. All data represent the mean ± SEM, and *$p < 0.05$.
(F) Representative epifluorescence images from HEK293 cells transfected with WT Kv7.5 or the identified channel mutant. Hoescht 33342 labeling of nuclei is in blue, and Kv7.5 channel staining is in white.
(G) Mean relative fluorescence intensity measured from two to five images as in (F). Fluorescence values relative to those of WT Kv7.5 were 0.55 ± 0.07 for p.Val145Gly, 0.60 ± 0.02 for p.Leu341Ile, 0.96 ± 0.04 for p.Pro369Arg, and 0.89 ± 0.04 for p.Ser448Ile.
All data shown are presented as the mean ± SEM.

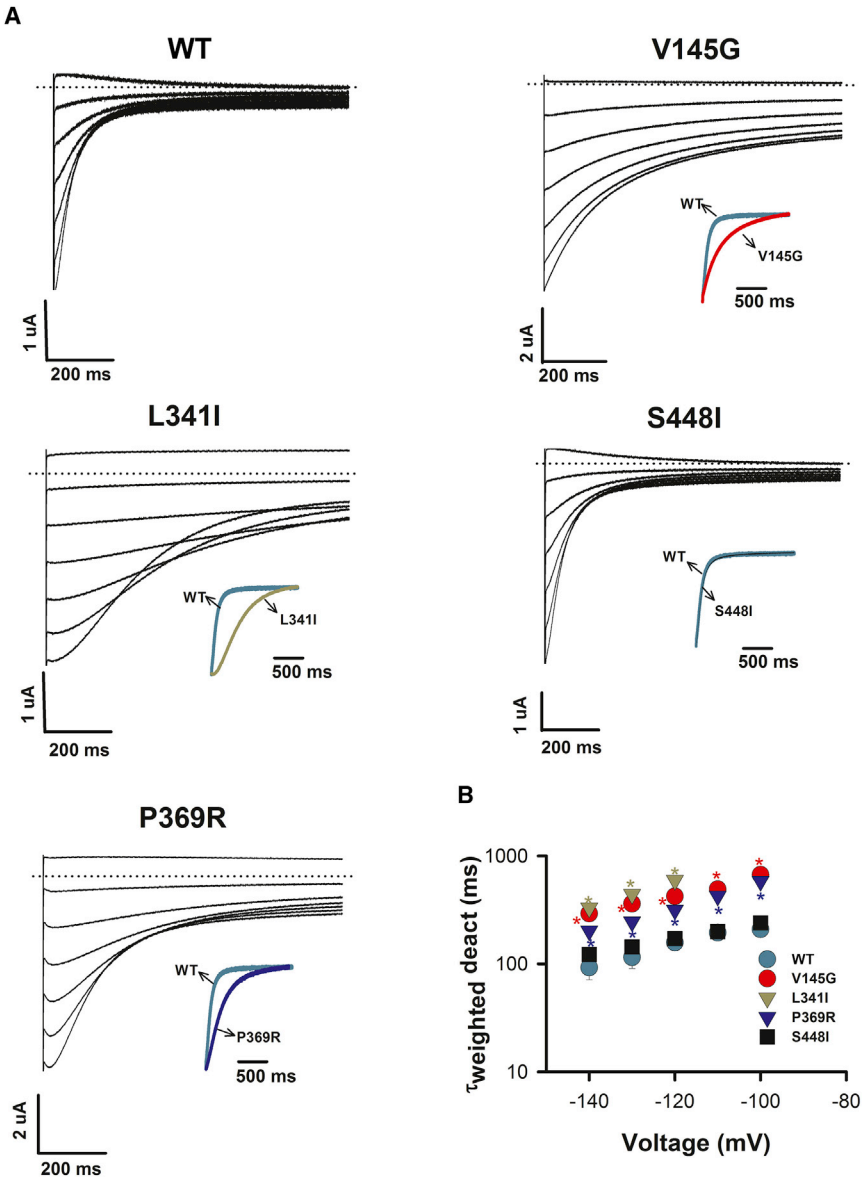

Figure 3. Deactivation Gating of Homomeric WT and Mutant Kv7.5 Channels

(A) Representative deactivating tail current traces for WT, p.Val145Gly (V145G), p.Leu341Ile (L341I), p.Ser448Ile (S448I), and p.Pro369Arg (P369R) Kv7.5 were recorded in *Xenopus laevis* oocytes during a range of test voltages applied after a 3 s depolarization step to 0 mV to activate channels. The inset shows the superposition of normalized tail current traces from WT and mutant Kv7.5 channels recorded at −140 mV to highlight the change in deactivation.

(B) Deactivation kinetics for WT and mutant channels. Tail current decays were fitted to a double exponential function to yield the values for τ_{fast} and τ_{slow} of deactivation. Mean $\tau_{weighted}$ (derived from the sum of τ_{fast} and τ_{slow} weighted according the relative amplitude of each component) of the deactivating currents were plotted over a range of voltages. All data represent the mean ± SEM, and $^{*}p < 0.05$.

All data shown are presented as the mean ± SEM.

action-potential firing during long-lasting depolarizing inputs. Inhibition of M-currents leads to enhanced neuronal excitability associated with a wide spectrum of early-onset epileptic disorders ranging from benign familial neonatal convulsions to severe epileptic encephalopathies and/or intellectual disability.[25] A dominant-negative *Kcnq5* mutation in mice has been shown to alter synaptic inhibition and excitability in the hippocampus, an area of high expression, although seizures were not observed.[26,27]

Given this background, we hypothesized that M-current could be adversely affected by *KCNQ5* mutations and sought electrophysiologic confirmation. *Xenopus laevis* oocytes are a useful model system given that heterologous expression of *KCNQ2* and *KCNQ3* has been shown to recapitulate the biophysical and pharmacological profile of native M-currents.[28] Electrophysiological characterization of mutant and WT channels in the heterologous expression system of *Xenopus* oocytes showed that these four *KCNQ5* mutations all alter channel gating properties, producing a loss-of-function phenotype in three cases and a gain of function in another case (c.1106C>G [p.Pro369Arg]). The obtained results suggest that the primary consequence of *KCNQ5* mutations is a change in the gating properties of M-channels.

The most pronounced phenotypic disturbance was observed in p.Pro369Arg channels, present in the most severely affected child, individual 4. Compared with the WT, p.Pro369Arg stabilized the activated state of the channel (left shifted the activation curve; Figure 2B), accelerated activation kinetics (Figure 2C and D), and slowed deactivation kinetics (Figure 3B), in keeping with a straightforward gain of function in the mutant channels. This effect is strikingly similar to the action of the Kv7-channel-activator compound, retigabine, which induces a pronounced left shift of the activation-voltage relationship in M-currents recorded from sympathetic neurons.[29] Increased function of M-currents has been suggested to increase neuronal excitability,[7] which could be due to overactivation of hyperpolarization-activated non-selective cation channels, resulting in secondary depolarizations.[30] The dramatic stabilization of activated states in comparison with closed states, induced by Kv7.5 p.Pro369Arg, is predicted to increase excitability and helps explain the severe phenotype of individual 4. It is also of interest to note the strikingly different seizure phenotypes between individuals 4 and 1, the former of whom

has infantile spasms and tonic seizures and the latter of whom has focal-onset seizures with impaired awareness.

The p.Val145Gly and p.Leu341Ile alterations resulted in a depolarizing shift of the activation curve (Figure 2B) accompanied by a dramatic slowing of early activation kinetics (Figure 2C). Furthermore, channel expression was significantly reduced in both cases. These effects are characteristic of a loss-of-function effect.[22–24] The severity of the loss-of-function phenotype in these mutant channels is possibly lessened by the slowed deactivation kinetics caused by the mutations, which would be predicted to increase repolarizing currents and reduce action-potential firing; however, the reduced channel expression would be expected to dominate. Channels with p.Ser448Ile also slowed the kinetics of early activation and are therefore likely to produce a loss of function. This variant did not alter channel expression and had the mildest effect of the four variants studied. Consistent with previous findings on *KCNQ2* mutations,[22] reduced function of Kv7.5 channels resulting from these variants is predicted to cause a lowered seizure threshold as a result of decreased neuronal repolarization reserve mediated by the M-current.

From a structure-function perspective, it is interesting that variants in the S6 pore and C terminus, as well as within the voltage-sensing unit (S1), modify the voltage dependence of activation gating and/or its kinetics. The effect of p.Pro369Arg, in particular, suggests that the proximal C-terminal region can dramatically influence the stability of the open state of these channels. It is also interesting that activation and deactivation gating are apparently independently altered by p.Val145Gly and p.Leu341Ile; in these cases, both activation and deactivation were slowed, suggesting that these processes are independently influenced by the variants.

The effects of co-assembly of altered subunits and WT Kv7.5 subunits have yet to be explored. Kv7.5 subunits might also co-assemble with Kv7.3 subunits in vivo to contribute to the M-current,[8,21] as well as *KCNE1* and *KCNE3* (MIM: 604433), which are endogenously expressed in *Xenopus* oocytes, and we have not explored the effect of the de novo mutations in such protein complexes.

Our data demonstrate that *KCNQ5* mutations that interfere with channel function most likely cause a congenital neurodevelopmental disorder with phenotypes of nonsyndromic intellectual disability or epileptic encephalopathy. The experimental and in silico evidence is particularly strong for c.434T>G (p.Val145Gly), c.1021C>A (p.Leu341Ile), and c.1106C>G (p.Pro369Arg) and less so for c.1343G>T (p.Ser448Ile). Future research should explore genetically and structurally informed pharmacological interventions.

Consortia

Investigators in the CAUSES study include Shelin Adam, Christèle du Souich, Alison M. Elliott, Anna Lehman, Jill Mwenifumbo, Tanya N. Nelson, Clara van Karnebeek, and Jan M. Friedman.

Investigators in the EPGEN study include Shelin Adam, Cyrus Boelman, Corneliu Bolbocean, Sarah E. Buerki, Tara Candido, Patrice Eydoux, Daniel M. Evans, William Gibson, Gabriella Horvath, Linda Huh, Tanya N. Nelson, Graham Sinclair, Tamsin Tarling, Eric B. Toyota, Katelin N. Townsend, Margot I. Van Allen, Clara van Karnebeek, and Suzanne Vercauteren.

Conflicts of Interest

In accordance with ethical obligation as researchers, co-authors K.M. and R.P. report that they are employees of GeneDx Inc., a wholly owned subsidiary of OPKO Health Inc., a company that could be affected by the research reported in this paper. They have disclosed these interests to the publisher and have in place an approved plan for managing any potential conflicts arising from such employment. M.B.C. received research grants and/or speakers' honoraria from the University of British Columbia, Novartis, Biocodex, Eisai, and Sage Therapeutics. Honoraria are donated to the Epilepsy Research and Development Fund.

Acknowledgments

We thank the families for participating in this research. We thank the British Columbia Children's Hospital (BCCH) BioBank, which is supported by Mining for Miracles through the BCCH Foundation. The bioinformatic pipeline used in the CAUSES study was developed in the laboratory of Wyeth Wasserman with intellectual contributions from Dave Arenillas, Phillip Richmond, Casper Shyr, Alison Matthews, and Maja Tarailo-Graovac. We are grateful for assistance from the BCCH Department of Pathology & Laboratory Medicine and the BCCH Electroencephalography Department. We thank Ji Qi and Jacob Kemp for expert technical assistance with functional-characterization experiments. The CAUSES study is funded by Mining for Miracles (BCCH Foundation) and Genome British Columbia with support from the British Columbia Provincial Health Services Authority and British Columbia Women's Hospital. Functional studies were funded by the Rare Disease Foundation and a Natural Sciences and Engineering Research Council of Canada Discovery Grant. EPGEN is funded by the Canada Excellence Research Chair, Leading Edge Endowment Fund, Rare Disease Foundation, Grocholski Foundation, and Alva Foundation.

Received: February 21, 2017
Accepted: May 24, 2017
Published: June 29, 2017

Web Resources

CAUSES Clinic, http://www.causes.clinic
ClinVar GeneDx, https://www.ncbi.nlm.nih.gov/clinvar/submitters/26957/
Clustal Omega, http://www.clustal.org/
ExAC Browser, http://exac.broadinstitute.org/
GenBank, https://www.ncbi.nlm.nih.gov/genbank/
GeneMatcher, https://genematcher.org/
gnomAD, http://gnomad.broadinstitute.org/
MutationTaster, http://www.mutationtaster.org/
NHLBI Exome Sequencing Project (ESP) Exome Variant Server, http://evs.gs.washington.edu/EVS/

OMIM, http://omim.org
PROVEAN, http://provean.jcvi.org/
REVEL: Rare Exome Variant Ensemble Learner, https://sites.google.com/site/revelgenomics/
SIFT, http://sift.jcvi.org/
UCSC Genome Browser, http://genome.ucsc.edu/
UniProt, http://www.uniprot.org/

References

1. Coetzee, W.A., Amarillo, Y., Chiu, J., Chow, A., Lau, D., McCormack, T., Moreno, H., Nadal, M.S., Ozaita, A., Pountney, D., et al. (1999). Molecular diversity of K+ channels. Ann. N Y Acad. Sci. *868*, 233–285.
2. Wang, Q., Curran, M.E., Splawski, I., Burn, T.C., Millholland, J.M., VanRaay, T.J., Shen, J., Timothy, K.W., Vincent, G.M., de Jager, T., et al. (1996). Positional cloning of a novel potassium channel gene: KVLQT1 mutations cause cardiac arrhythmias. Nat. Genet. *12*, 17–23.
3. Neyroud, N., Tesson, F., Denjoy, I., Leibovici, M., Donger, C., Barhanin, J., Fauré, S., Gary, F., Coumel, P., Petit, C., et al. (1997). A novel mutation in the potassium channel gene KVLQT1 causes the Jervell and Lange-Nielsen cardioauditory syndrome. Nat. Genet. *15*, 186–189.
4. van Vliet-Ostaptchouk, J.V., van Haeften, T.W., Landman, G.W.D., Reiling, E., Kleefstra, N., Bilo, H.J.G., Klungel, O.H., de Boer, A., van Diemen, C.C., Wijmenga, C., et al. (2012). Common variants in the type 2 diabetes KCNQ1 gene are associated with impairments in insulin secretion during hyperglycaemic glucose clamp. PLoS ONE *7*, e32148.
5. Singh, N.A., Charlier, C., Stauffer, D., DuPont, B.R., Leach, R.J., Melis, R., Ronen, G.M., Bjerre, I., Quattlebaum, T., Murphy, J.V., et al. (1998). A novel potassium channel gene, KCNQ2, is mutated in an inherited epilepsy of newborns. Nat. Genet. *18*, 25–29.
6. Charlier, C., Singh, N.A., Ryan, S.G., Lewis, T.B., Reus, B.E., Leach, R.J., and Leppert, M. (1998). A pore mutation in a novel KQT-like potassium channel gene in an idiopathic epilepsy family. Nat. Genet. *18*, 53–55.
7. Miceli, F., Striano, P., Soldovieri, M.V., Fontana, A., Nardello, R., Robbiano, A., Bellini, G., Elia, M., Zara, F., Taglialatela, M., and Mangano, S. (2015). A novel KCNQ3 mutation in familial epilepsy with focal seizures and intellectual disability. Epilepsia *56*, e15–e20.
8. Lerche, C., Scherer, C.R., Seebohm, G., Derst, C., Wei, A.D., Busch, A.E., and Steinmeyer, K. (2000). Molecular cloning and functional expression of KCNQ5, a potassium channel subunit that may contribute to neuronal M-current diversity. J. Biol. Chem. *275*, 22395–22400.
9. Kubisch, C., Schroeder, B.C., Friedrich, T., Lütjohann, B., El-Amraoui, A., Marlin, S., Petit, C., and Jentsch, T.J. (1999). KCNQ4, a novel potassium channel expressed in sensory outer hair cells, is mutated in dominant deafness. Cell *96*, 437–446.
10. Sobreira, N., Schiettecatte, F., Valle, D., and Hamosh, A. (2015). GeneMatcher: a matching tool for connecting investigators with an interest in the same gene. Hum. Mutat. *36*, 928–930.
11. Tarailo-Graovac, M., Shyr, C., Ross, C.J., Horvath, G.A., Salvarinova, R., Ye, X.C., Zhang, L.-H., Bhavsar, A.P., Lee, J.J.Y., Drögemöller, B.I., et al. (2016). Exome Sequencing and the Management of Neurometabolic Disorders. N. Engl. J. Med. *374*, 2246–2255.
12. Tanaka, A.J., Cho, M.T., Millan, F., Juusola, J., Retterer, K., Joshi, C., Niyazov, D., Garnica, A., Gratz, E., Deardorff, M., et al. (2015). Mutations in SPATA5 Are Associated with Microcephaly, Intellectual Disability, Seizures, and Hearing Loss. Am. J. Hum. Genet. *97*, 457–464.
13. Demos, M., Guella, I., McKenzie, M.B., Buerki, S.E., Evans, D.M., Toyota, E.B., Boelman, C., Huh, L.L., Datta, A., Michoulas, A., et al. (2017). Diagnostic Yield and Treatment Impact of Targeted Exome Sequencing in Early-onset Epilepsy. bioRxiv. https://doi.org/10.1101/139329.
14. Ioannidis, N.M., Rothstein, J.H., Pejaver, V., Middha, S., McDonnell, S.K., Baheti, S., Musolf, A., Li, Q., Holzinger, E., Karyadi, D., et al. (2016). REVEL: An Ensemble Method for Predicting the Pathogenicity of Rare Missense Variants. Am. J. Hum. Genet. *99*, 877–885.
15. Lek, M., Karczewski, K.J., Minikel, E.V., Samocha, K.E., Banks, E., Fennell, T., O'Donnell-Luria, A.H., Ware, J.S., Hill, A.J., Cummings, B.B., et al.; Exome Aggregation Consortium (2016). Analysis of protein-coding genetic variation in 60,706 humans. Nature *536*, 285–291.
16. Tarpey, P.S., Smith, R., Pleasance, E., Whibley, A., Edkins, S., Hardy, C., O'Meara, S., Latimer, C., Dicks, E., Menzies, A., et al. (2009). A systematic, large-scale resequencing screen of X-chromosome coding exons in mental retardation. Nat. Genet. *41*, 535–543.
17. Lelieveld, S.H., Reijnders, M.R.F., Pfundt, R., Yntema, H.G., Kamsteeg, E.-J., de Vries, P., de Vries, B.B.A., Willemsen, M.H., Kleefstra, T., Löhner, K., et al. (2016). Meta-analysis of 2,104 trios provides support for 10 new genes for intellectual disability. Nat. Neurosci. *19*, 1194–1196.
18. Deciphering Developmental Disorders Study (2017). Prevalence and architecture of de novo mutations in developmental disorders. Nature *542*, 433–438.
19. Iossifov, I., O'Roak, B.J., Sanders, S.J., Ronemus, M., Krumm, N., Levy, D., Stessman, H.A., Witherspoon, K.T., Vives, L., Patterson, K.E., et al. (2014). The contribution of de novo coding mutations to autism spectrum disorder. Nature *515*, 216–221.
20. Greene, D.L., and Hoshi, N. (2017). Modulation of Kv7 channels and excitability in the brain. Cell. Mol. Life Sci. *74*, 495–508.
21. Schroeder, B.C., Hechenberger, M., Weinreich, F., Kubisch, C., and Jentsch, T.J. (2000). KCNQ5, a novel potassium channel broadly expressed in brain, mediates M-type currents. J. Biol. Chem. *275*, 24089–24095.
22. Castaldo, P., del Giudice, E.M., Coppola, G., Pascotto, A., Annunziato, L., and Taglialatela, M. (2002). Benign familial neonatal convulsions caused by altered gating of KCNQ2/KCNQ3 potassium channels. J. Neurosci. *22*, RC199.
23. Hunter, J., Maljevic, S., Shankar, A., Siegel, A., Weissman, B., Holt, P., Olson, L., Lerche, H., and Escayg, A. (2006). Subthreshold changes of voltage-dependent activation of the K(V)7.2 channel in neonatal epilepsy. Neurobiol. Dis. *24*, 194–201.
24. Orhan, G., Bock, M., Schepers, D., Ilina, E.I., Reichel, S.N., Löffler, H., Jezutkovic, N., Weckhuysen, S., Mandelstam, S., Suls, A., et al. (2014). Dominant-negative effects of KCNQ2 mutations are associated with epileptic encephalopathy. Ann. Neurol. *75*, 382–394.
25. Weckhuysen, S., Mandelstam, S., Suls, A., Audenaert, D., Deconinck, T., Claes, L.R.F., Deprez, L., Smets, K., Hristova, D., Yordanova, I., et al. (2012). KCNQ2 encephalopathy: emerging phenotype of a neonatal epileptic encephalopathy. Ann. Neurol. *71*, 15–25.

26. Fidzinski, P., Korotkova, T., Heidenreich, M., Maier, N., Schuetze, S., Kobler, O., Zuschratter, W., Schmitz, D., Ponomarenko, A., and Jentsch, T.J. (2015). KCNQ5 K(+) channels control hippocampal synaptic inhibition and fast network oscillations. Nat. Commun. *6*, 6254.
27. Tzingounis, A.V., Heidenreich, M., Kharkovets, T., Spitzmaul, G., Jensen, H.S., Nicoll, R.A., and Jentsch, T.J. (2010). The KCNQ5 potassium channel mediates a component of the afterhyperpolarization current in mouse hippocampus. Proc. Natl. Acad. Sci. USA *107*, 10232–10237.
28. Wang, H.-S., Pan, Z., Shi, W., Brown, B.S., Wymore, R.S., Cohen, I.S., Dixon, J.E., and McKinnon, D. (1998). KCNQ2 and KCNQ3 potassium channel subunits: molecular correlates of the M-channel. Science *282*, 1890–1893.
29. Brown, D.A., and Passmore, G.M. (2009). Neural KCNQ (Kv7) channels. Br. J. Pharmacol. *156*, 1185–1195.
30. Hu, H., Vervaeke, K., Graham, L.J., and Storm, J.F. (2009). Complementary theta resonance filtering by two spatially segregated mechanisms in CA1 hippocampal pyramidal neurons. J. Neurosci. *29*, 14472–14483.